Author/s:
Chandrasekar, K;Farrugia, BL;Johnson, L;Marks, D;Irving, D;Elgundi, Z;Lau, K;Kim, HN;Rnjak-Kovacina, J;Bilek, MM;Whitelock, JM;Lord, MS

Title:
Effect of Recombinant Human Perlecan Domain V Tethering Method on Protein Orientation and Blood Contacting Activity on Polyvinyl Chloride

Date:
2021-07-01

Citation:
Chandrasekar, K., Farrugia, B. L., Johnson, L., Marks, D., Irving, D., Elgundi, Z., Lau, K., Kim, H. N., Rnjak-Kovacina, J., Bilek, M. M., Whitelock, J. M. & Lord, M. S. (2021). Effect of Recombinant Human Perlecan Domain V Tethering Method on Protein Orientation and Blood Contacting Activity on Polyvinyl Chloride. Advanced Healthcare Materials, 10 (14), https://doi.org/10.1002/adhm.202100388.

Effect of recombinant human perlecan domain V tethering method on protein orientation and blood contacting activity on polyvinyl chloride

*Keerthana Chandrasekar, Brooke L. Farrugia, Lacey Johnson, Denese Marks, David Irving, Zehra Elgundi#, Kieran Lau, Ha Na Kim, Jelena Rnjak-Kovacina, Marcela M. Bilek, John M. Whitelock, Megan S. Lord**

Dr. K. Chandrasekar, Dr. Z. Elgundi, K. Lau, H. Kim, Dr. J. Rnjak-Kovacina, Prof. J.M. Whitelock, Assoc. Prof. M.S. Lord

Graduate School of Biomedical Engineering, UNSW Sydney, Sydney NSW 2052, Australia
E-mail: m.lord@unsw.edu.au

Dr. B.L. Farrugia
Department of Biomedical Engineering, Melbourne School of Engineering, The University of Melbourne, Melbourne VIC 3010, Australia

Dr. L. Johnson, Dr. D. Marks, Dr. D. Irving

Australian Red Cross Lifeblood, Alexandria NSW 2015, Australia

Prof. M.M. Bilek

The Charles Perkins Centre, University of Sydney, NSW 2006, Australia

The University of Sydney Nano Institute, University of Sydney, NSW 2006, Australia

School of Physics, University of Sydney, Sydney, NSW 2006, Australia

School of Biomedical Engineering, University of Sydney, Sydney, NSW 2006, Australia

Keywords: polyvinyl chloride, perlecan, extracellular matrix, platelet, blood, plasma immersion ion implantation

Surface modification of biomaterials is a promising approach to control biofunctionality whilst retaining the bulk biomaterial properties. Perlecan is the major proteoglycan in the vascular basement membrane that supports low levels of platelet adhesion but not activation. Thus, perlecan is a promising bioactive for blood-contacting applications. This study furthers the mechanistic understanding of platelet interactions with perlecan by establishing that platelets utilize domains III and V of the core protein for adhesion. Polyvinyl chloride (PVC) is functionalized with recombinant human perlecan domain V (rDV) to explore the effect of the tethering method on proteoglycan orientation and bioactivity. Tethering of rDV to PVC is achieved via either physisorption or covalent attachment via plasma immersion ion implantation (PIII) treatment. Both methods of rDV tethering reduce platelet adhesion and activation compared to the pristine PVC, however, the mechanisms are unique for each tethering method. Physisorption of rDV on PVC orientates the molecule to hinder access to the integrin-binding region which inhibits platelet adhesion. In contrast, PIII treatment orientates rDV to allow access to the integrin-binding region which is rendered anti-adhesive to platelets via the glycosaminoglycan (GAG) chain. These effects demonstrate the potential of rDV biofunctionalization to modulate platelet interactions for blood contacting applications.

1. Introduction

The incorporation of biomolecules, such as proteins, into biomaterials via surface modification is increasingly explored to design biomaterials that interface with the biological environment for successful clinical outcomes. Purely synthetic materials with desirable biological cues can be difficult to realize while the incorporation of biomolecules, which define almost all biological processes, has gained popularity in biomaterials design. There are a range of tethering methods for pristine or modified biomolecules currently under investigation and these can be categorized into physical adsorption (physisorption) or covalent attachment.[1-3] Physisorption cannot ensure persistence due to the propensity of physisorbed biomolecules to be displaced by other molecules in the complex biological environment.[4, 5] Typically covalent tethering is achieved using complex multi-step wet chemistry, which has the potential to lead to unintended side reactions, cytotoxicity, and may also interfere with the biological activity of the immobilized biomolecules. More recently, covalent tethering was achieved on polymeric surfaces by a reagent-free approach which relies on reactions with radicals embedded in the surface by an energetic ion pretreatment known as plasma immersion ion implantation (PIII).[6] This pretreatment also renders polymeric surfaces hydrophilic which enables the subsequently tethered biomolecules to retain their native conformation and thus remain functional.[7]

Polyvinyl chloride (PVC) incorporating a plasticizer, such as di-2-ethylhexyl phthalate (DEHP), is one of the most widely used polymeric biomaterials in medical devices including blood component storage bags, extracorporeal circuits, intravenous catheters and endotracheal tubes due to its transparency, flexibility, chemical resistance and ease of sterilization.[8-10] Each of these are short-term, single-use applications due to the propensity of PVC to support non-specific protein

adsorption, activation of clotting factors and cell adhesion that can lead to impaired biological performance, such as thrombosis.[11, 12] Furthermore, PVC does not support endothelial cell adhesion or proliferation[13], precursors to biomaterial endothelialization which is a recognized requirement for long-term performance of implanted blood-contacting biomaterials.[14] Surface modification of PVC for these applications via wet chemical methods relies on modification via hydrolysis, oxidation or aminolysis and have been used to tether biomolecules such as heparin, alginate, dextran and hyaluronan[15, 16] or synthetic polymer brushes such as poly(N,N-dimethylacrylamide)[17] and polyethylene glycol.[18] Alternatively, plasma or UV treatment can be used for surface activation of PVC followed by functionalization with anti-bacterial compounds,[19-24] synthetic polymers such as poly(carboxybetaine) and poly(oligo(ethylene glycol) methyl ether acrylate)[25] or biomolecules such as albumin[26] or chitosan[27, 28] for blood contacting applications. However, PIII is yet to be explored for the immobilization of biomolecules on PVC capable of modulating vascular cell bioactivity.

Various biomolecules that resist platelet adhesion have been explored as biomaterial coatings, most notably albumin and heparin. Interestingly, most proteins present in the vascular wall, including collagen, laminin, fibronectin and vitronectin, activate platelets, while elastin and perlecan do not.[29-32] Albumin is the most abundant plasma protein which can reduce platelet adhesion when coated on many biomaterials.[33] However, it is prone to conformational change upon adsorption, which can affect its ability to resist platelet adhesion.[34, 35] Furthermore, while albumin inhibits vascular smooth muscle cell adhesion,[36] it does not support endothelial cell adhesion;[37] a key cell type at the interface of native blood vessels that enables long-term applications of blood-contacting biomaterials via surface endothelialization. Heparin has been widely studied for blood-contacting

applications due to its anticoagulant activity and exploited for applications such as hemodialysis catheters, vascular grafts and coronary stents.[38] However, heparin coatings in these applications have not achieved improved clinical performance over the pristine biomaterial which may in part be due to structural modification with immobilization.[39, 40] In addition, platelet factor 4 can bind to heparin which alters its structure and elicits an immune response resulting in the formation of antibodies that bind to the surface of platelets and cause platelet activation and aggregation; a life-threatening condition called heparin-induced thrombocytopenia.[31, 41]

Perlecan is the major proteoglycan of the vascular basement membrane, where it plays essential roles in vasculogenesis, angiogenesis and wound healing.[42-44] Perlecan contains five protein domains with glycosaminoglycan (GAG) chain attachment sites located in domains I and V which sequester, store and potentiate the signaling of a range of growth factors.[45, 46] In contrast to other bioactive molecules explored for blood-contacting applications, perlecan supports endothelial adhesion and proliferation while inhibiting the adhesion of smooth muscle cells and platelets.[36, 47] Furthermore, platelets are not activated by perlecan and perlecan can suppress platelet factor 4-mediated platelet activation.[31, 47] This vascular cell selectivity has also been demonstrated *in vivo* in a sheep carotid interposition model where perlecan coated expanded polytetrafluoroethylene grafts promoted endothelialization and reduced platelet adhesion compared to uncoated grafts.[48] Recombinant human perlecan domain V (rDV), which contains a single GAG site decorated with either chondroitin sulfate (CS) or heparan sulfate (HS) and an $\alpha_2\beta_1$ integrin binding site, can recapitulate the activities of full-length perlecan by supporting endothelial cell adhesion and

angiogenesis via potentiation of growth factor signaling.[36, 45, 47, 49, 50] In addition, rDV does not support smooth muscle cell adhesion[36] and supports a low level of platelet adhesion.[49, 51]

Although it is firmly established that rDV can play essential roles in the control of vascular cell function and is a promising bioactive molecule for modulation of vascular cell activities at the blood-biomaterial interface, the utility of immobilized forms of this molecule have only been explored on silk fibroin biomaterials.[49-51] The current study aimed to determine the regions of perlecan involved in platelet interactions and were found to reside within domains III and V (**Figure 1A**). Additionally, rDV was tethered to PVC using either physisorption or PIII treatment (**Figure 1B**) with the aim of establishing the effect of tethering method on protein orientation and mechanisms of platelet interactions in clinically relevant protein-containing plasma (plasma/SSP+) or protein-free (Tyrode's buffer) environments (**Figure 1C**) toward development of biofunctionalized surfaces for blood-contacting applications.

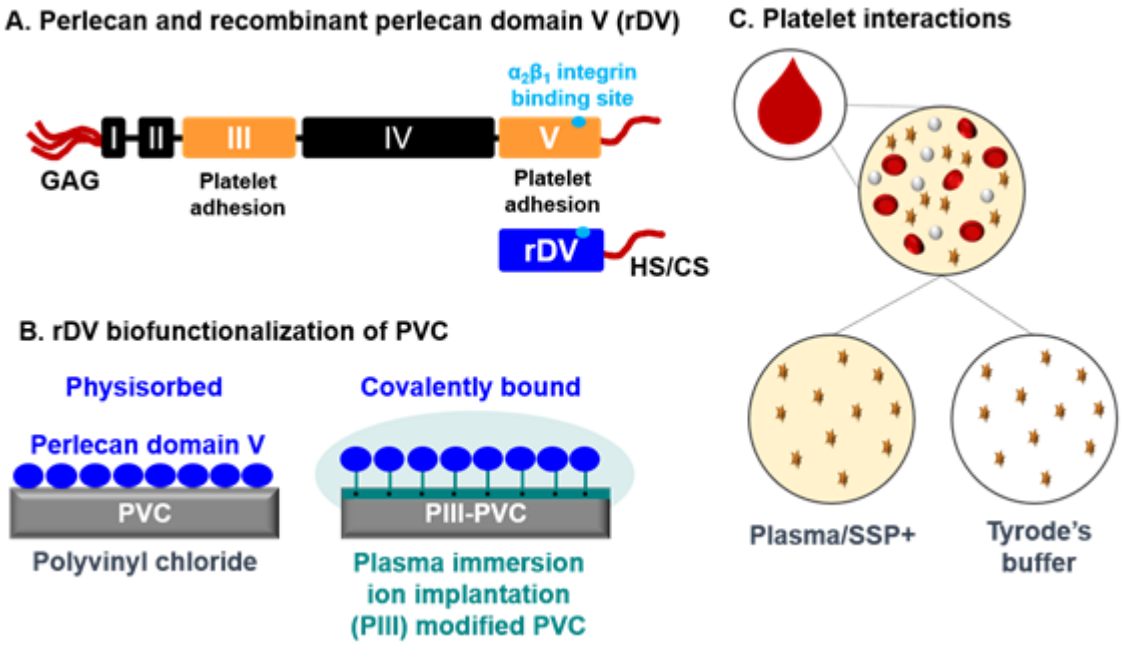

Figure 1. Schematic of study design elucidating the involvement of perlecan domains III and V in platelet adhesion and investigation of platelet interactions with recombinant human perlecan domain V (rDV) in solution and when biofunctionalized on PVC. (A) Schematic representation of perlecan containing 5 protein domains with glycosaminoglycan (GAG) attachment sites located in domains I and V and an $\alpha_2\beta_1$ integrin binding site located in domain V. In this study, platelet adhesion sites were found to reside within domains III and V. Schematic representation of rDV containing a glycosaminoglycan attachment site that is decorated with either heparan sulfate (HS) or chondroitin sulfate (CS). **(B)** Methods of tethering rDV to PVC via either physisorption or plasma immersion ion implantation (PIII). **(C)** Platelet interaction assays with rDV in solution or tethered to PVC in clinically relevant environments including protein-containing plasma (plasma/SSP+) or protein-free (Tyrode's buffer) environments.

2. Results

2.1. Platelets adhere to perlecan core protein via domains III and V

The ability of perlecan to support platelet adhesion, a key process in thrombogenesis, was studied *in vitro* using isolated human platelets suspended in Tyrode's buffer. Perlecan supported a low level of platelet adhesion, similar to that of the negative control, albumin, and 9.7-fold less than the positive control, fibrinogen (p<0.0001) (**Figure 2A and B)**. In the absence of GAG chains, platelet adhesion increased by 2-fold on the perlecan core protein, compared to the proteoglycan form (p=0.0440) (Figure 2A and B). To explore the domains of perlecan involved in platelet adhesion, the core protein was pre-incubated with monoclonal antibodies to either domains I, III, IV or V prior to exposure to platelets (**Figure 2C)**. The addition of antibodies to either domains III or V reduced platelet adhesion 2.3- and 5.7-fold, respectively (p=0.0075 and 0.0005, respectively), compared to in the absence of antibodies (**Figure 2D**), indicating that these regions were involved in platelet adhesion. While there is a risk that an antibody will non-specifically interfere with platelet adhesion, this effect would be expected for each of the antibodies. However, the anti-domain I and IV antibodies had no effect on the level of platelet adhesion compared to the control (p>0.05), supporting the integrity of the assay.

Platelet adhesion to the perlecan core protein was further explored by the addition of peptides as decoys (**Figure 2E**). Peptides from each of the domains of perlecan were chosen based on bioinformatics and structural modeling which predicted peptide motifs within each domain likely exposed allowing for platelet interaction.[52] None of the domain-specific antibodies reacted with the peptides (data not shown). The sequence as well as the 3-dimensional structure of the peptides

likely affected their ability to react with the antibodies. Exposure of platelets to the peptides IIIa and IIIc derived from domain III prior to exposure to the perlecan core protein reduced platelet adhesion by 2.7- and 2.4-fold, respectively (p=0.0026 and 0.0050, respectively) (Figure 2E). Furthermore, peptide V derived from domain V of perlecan reduced platelet adhesion by 8.3-fold (p<0.0001). These data indicated that platelet adhesion to perlecan involved domains III and V of the core protein.

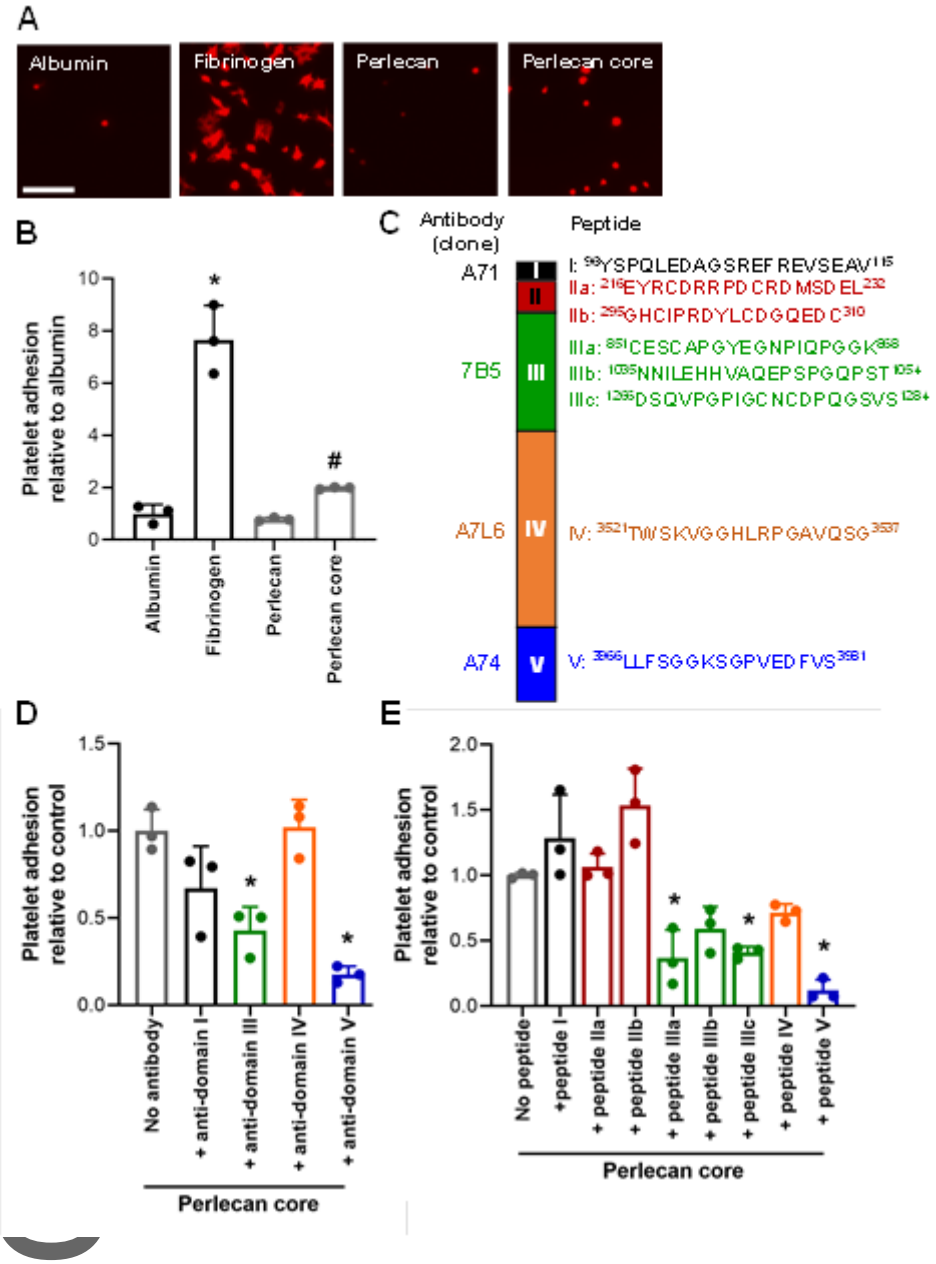

Figure 2. Platelets bind to perlecan via domains III and V. (A) Representative images of platelet adhesion to albumin, fibrinogen, perlecan or perlecan core protein immobilized on tissue culture plastic detected by fluorescence microscopy following actin staining using rhodamine phalloidin. Scale bar = 20 µm. **(B)** Quantification of images such as shown in (A) for platelet adhesion to

perlecan or perlecan core protein presented as fold change compared to albumin. Perlecan core protein was generated by heparinase III digestion of perlecan. Data are mean ± SD, *n*=3, *p*-values were calculated using one-way ANOVA with Tukey's test, **p*<0.05 compared to albumin and $^{\#}p$<0.05 compared to perlecan. **(C)** Schematic of perlecan core domains, the domain epitopes of the anti-perlecan antibodies and the location of peptides. **(D)** Platelet adhesion to perlecan core immobilized on chamber slides in the presence of antibodies to domain I (clone A71), domain III (clone 7B5), domain IV (clone A7L6) or domain V (clone A74) presented as fold change compared to no antibody (control). Data are mean ± SD, *n*=3, *p*-values were calculated using one-way ANOVA with Tukey's test, **p*<0.05 compared to control. (E) Platelet adhesion to perlecan core in the presence of peptides to domain I (I), domain II (IIa and IIb), domain III (IIIa, IIIb and IIIc), domain IV (IV) or domain V (V) presented as fold change compared to no peptide (control). Data are mean ± SD, *n*=3, *p*-values were calculated using one-way ANOVA with Tukey's test, **p*<0.05 compared to control.

2.2. rDV modulates platelet adhesion

While it might appear counter-intuitive to further explore platelet adhesion to domain V of perlecan, presentation of this domain alone has previously been shown to possess different bioactivity to full-length perlecan, such as resisting smooth muscle cell adhesion.[36] Furthermore, the ability of rDV to support endothelial cell, but not smooth muscle cell adhesion make it a promising bioactive coating for long-term blood-contacting applications and thus it was of interest to further explore its interactions with platelets. rDV supported a low level of platelet adhesion to the same extent as perlecan and albumin (p>0.05) (**Figure 3A**). However, in contrast to perlecan, removal of the GAGs, either HS, CS or both, from rDV did not enhance platelet adhesion (p>0.05), indicating its promise as a coating to modulate platelet adhesion. Higher resolution SEM imaging revealed extensive spreading of platelets adhered to fibrinogen (positive control) indicative of activation (**Figure 3B**). In contrast, platelets adhered on the perlecan core protein mostly exhibited late pseudopodial structures indicative of some activation, while platelets adhered on all forms of rDV exhibited a

discoid shape with few early pseudopodial structures similar to albumin, indicating low activation (Figure 3B). Thus, although rDV contains an integrin binding site, it is anti-adhesive for platelets when physisorbed on tissue culture plastic.

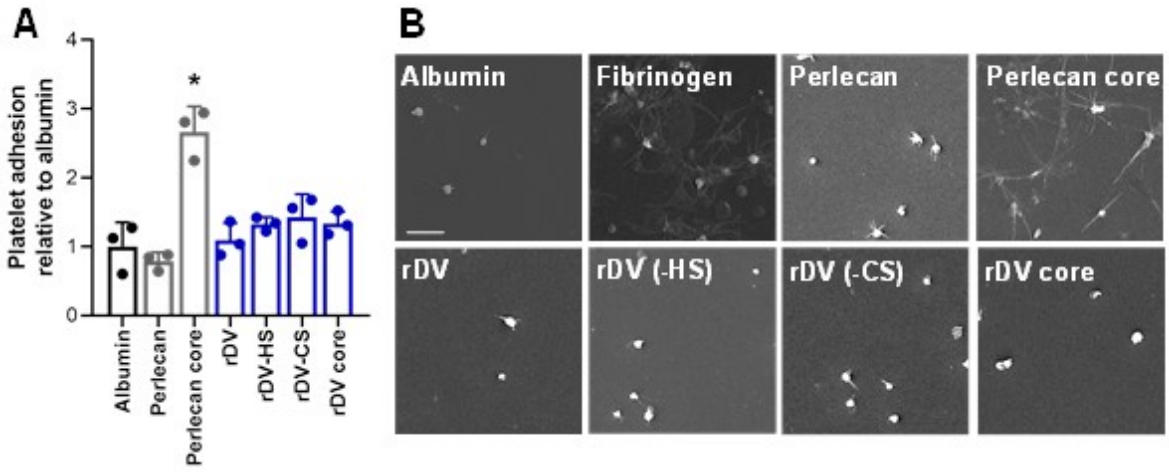

Figure 3. Platelet adhesion to rDV is independent of glycosaminoglycans. (A) Platelet adhesion to perlecan or rDV immobilized on tissue culture plastic presented as fold change compared to albumin. Perlecan core and rDV-HS were regenerated by heparinase III digestion of perlecan and rDV, respectively. rDV-CS was generated by chondroitinase ABC digestion of rDV and rDV core was generated by digestion with both heparinase III and chondroitinase ABC. Data are mean ± SD, n=3, p-values were calculated using one-way ANOVA with Tukey's test, *p<0.05 compared to albumin and perlecan. **(B)** Representative images of platelet adhesion to albumin, fibrinogen, perlecan or rDV immobilized on glass coverslips detected by scanning electron microscopy. Scale bar = 10 µm.

Further analysis of platelet activation with exposure to either perlecan or rDV was performed via measurement of platelet surface expression of P-selectin (or CD62P), a marker of activation only present on the platelet surface upon release from the α-granules inside platelets via activation.[53] Flow cytometry analysis of P-selectin expression revealed that exposure of platelets to ADP (positive control) increased P-selectin expression while neither perlecan nor rDV increased P-selectin expression over the no stimulus control (**Figure 4A**). Platelet activation leads to a conformational change in GPIIb/IIIa, which is recognized by the monoclonal antibody clone PAC-1, and an indicator of late-stage platelet activation.[54] Flow cytometry analysis of activated GPIIb/IIIa revealed that exposure of platelets to ADP (positive control) increased expression, while neither perlecan nor rDV increased GPIIb/IIIa activation over the no stimulus control (**Figure 4B**). In addition, removal of the GAGs did not alter the activation profile for platelets exposed to either perlecan or rDV (**Figure S1**). Together, the flow cytometry measurements indicated that rDV did not support platelet activation when presented in solution.

Platelet interactions with immobilized rDV were explored by QCM-D to measure real-time interactions including platelet adhesion, spreading and activation via platelet-protein contacts.[55-57] The selected protein was physisorbed onto a gold sensor surface, blocked with albumin and then exposed to platelets suspended in Tyrode's buffer (**Figure 4C**). Each platelet binding event is represented by a decrease in frequency (*f*), which is in turn related to the amount of mass deposited, accompanied by an increase in dissipation (D), which is related to the viscoelasticity of the immobilized layer. Comparison of the platelet interaction behavior to the different coatings was performed by plotting ΔD versus Δ*f* (D*f* plots; **Figure 4D**). These plots indicated extensive platelet

interactions and activation on fibrinogen (positive control) that resulted in the largest decrease in Δ*f* and increase in ΔD. In contrast, platelet interactions with albumin (negative control) resulted in little change in both Δ*f* and ΔD indicative of the profile of a non-adhesive surface for platelets that did not induce platelet activation. Platelets responded in a similar way to immobilized perlecan and rDV with decreases in Δ*f* and little change in ΔD indicative of dynamic platelet-protein contacts without activation. Interestingly, the Δ*f* values had a greater magnitude than for platelets exposed to albumin indicative of a higher level of platelet-protein contacts. Together these data indicated that rDV did not activate platelets when immobilized via physisorption.

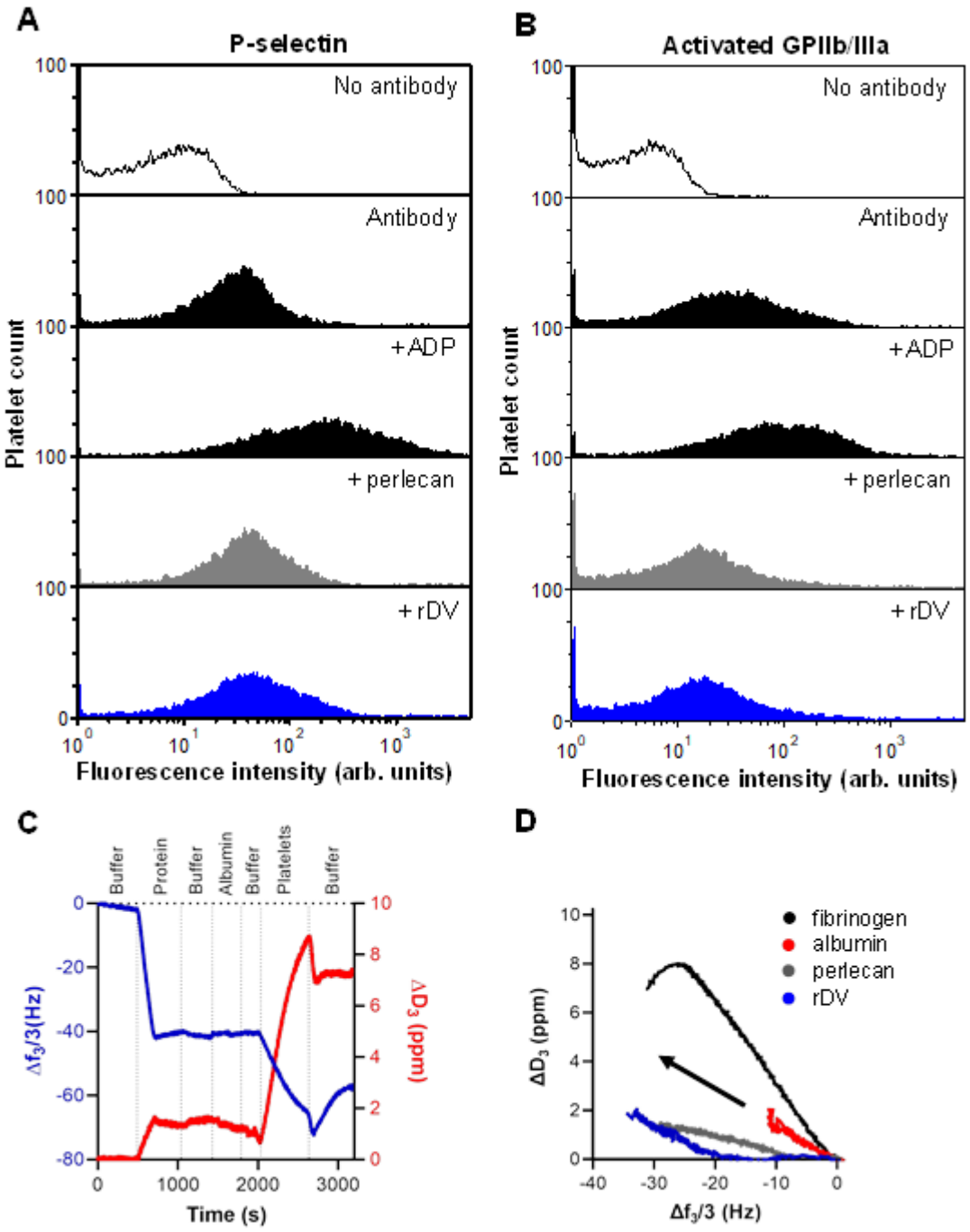

Figure 4. Platelets are not activated by rDV. Representative profiles of platelet surface expression of **(A)** P-selectin (CD62P) or **(B)** activated GPIIb/IIIa (antibody clone PAC-1) measured by flow cytometry after exposure to ADP, perlecan or rDV in solution. The profiles are representative of three independent experiments for each. **(C)** Sample QCM-D experiment of platelet binding to immobilized protein (fibrinogen) displayed as changes in frequency (Δf) and dissipation (ΔD) versus time for the third overtone. The vertical lines indicate the addition of PBS (buffer), protein, albumin or platelets. **(D)** Representative ΔD versus Δf plot (Df plots) for platelet binding to immobilized proteins. The arrow indicates the time course of the data points. The Df plots are representative of three independent experiments for each condition.

2.3 The orientation of rDV on PVC is affected by the tethering method

Next, rDV was explored as a molecule to biofunctionalize PVC to overcome the propensity of PVC to support cell interactions that can impair its biological performance.[11] While blood-contacting materials need to modulate the activities of a range of blood and blood vessel wall cell types, this study focused on platelets due to their propensity to rapidly adhere to synthetic biomaterials and support thrombogenesis[58] and built upon knowledge of the ability of rDV to support endothelial cells, but not vascular smooth muscle cells.[36, 45, 50] The biofunctionalization of PVC with rDV was explored by using either physisorption or physically modifying the surface of PVC using PIII to embed highly reactive radicals to facilitate direct covalent immobilization of rDV in the absence of chemical crosslinkers. PVC used in platelet storage bags that contains a micro-rough surface with circular features of ~ 200 µm diameter (**Figure 5A and B**) was used in this study. PIII treatment of PVC (PIII-PVC) yielded changes in the surface chemistry as observed by ATR-FTIR with increased intensity of absorption lines associated with OH, C=O, C=C and C-O bonds (**Figure 5C**), but not surface topography (**Figure S2**). Surface modification with PIII treatment was also evident by a reduced

water contact angle compared to PVC (p=0.0192, **Figure 5D**) indicative of a more hydrophilic surface than the untreated PVC.

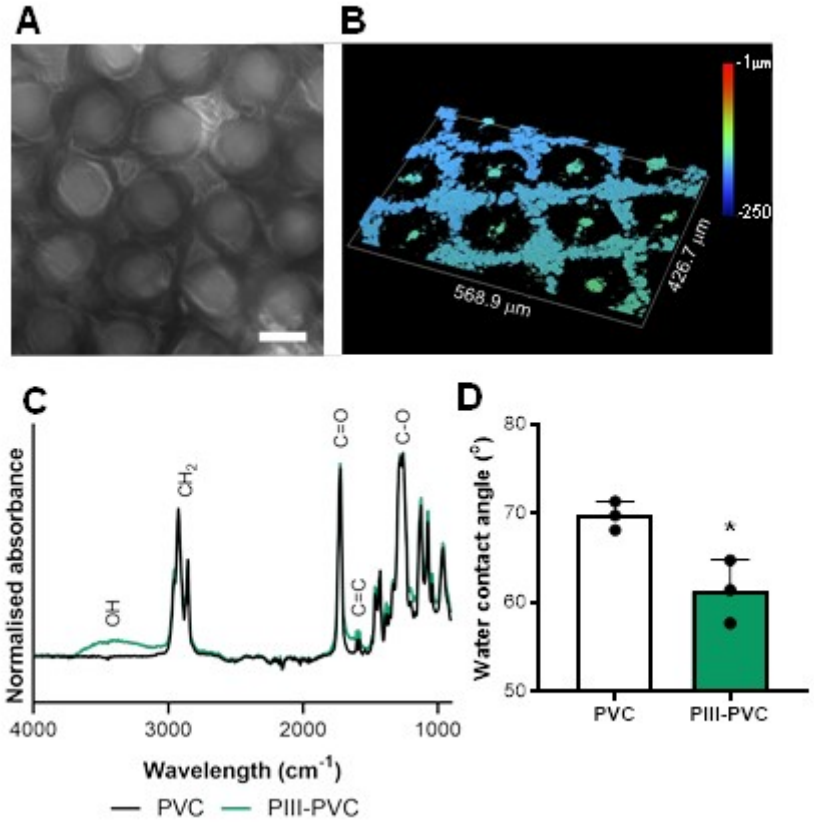

Figure 5. The surface of PVC is more hydrophilic after PIII treatment. (A) Optical microscope image of the surface of PVC. Scale bar = 100 µm. **(B)** Optical profile image of PVC. **(C)** ATR-FTIR spectra of PVC (black) and PVC 1 week after PIII treatment (PIII-PVC; green). **(D)** Contact angle measurement for PVC and PVC-PIII. Data are mean ± SD, n=3, p-values were calculated using one-way ANOVA with Tukey's test, *p<0.05 compared to PVC.

The ability of PIII-PVC to support robust tethering of rDV and its orientation was examined by ELISA using antibodies to epitopes within the core protein or GAG chains (**Figure 6A**). The strength of rDV binding to PVC and PIII-PVC was examined via the use of SDS, a detergent that interrupts the intermolecular interactions both within and between proteins and between proteins and a biomaterial surface.[59, 60] SDS treatment resulted in a 7.7-fold reduction (p<0.0001) in detectable rDV on PVC while there was no effect on PIII-PVC (**Figure 6B**). The same level of rDV was immobilized on PVC and PIII-PVC (p>0.05; Figure 6B) while fewer N-terminal epitopes were exposed for rDV immobilized on PIII-PVC than on PVC (p=0.0005; **Figure 6C**) and more C-terminal epitopes (p = 0.0017; **Figure 6D**). Additionally, the ratio of absorbance values for the N- to C-terminal epitopes indicated that rDV tethered to PVC favored exposure of the N-terminal epitopes while rDV tethered to PIII-PVC favored exposure of the C-terminal epitopes that contained the GAG attachment site and $\alpha_2\beta_1$ integrin binding site (p=0.0002; **Figure 6E**). In addition, while there was no effect of PIII treatment on the availability of the CS chain epitopes for immobilized rDV (p>0.05), there was a 1.73-fold reduction (p=0.0179) in HS chain epitopes for rDV tethered to PIII-PVC compared to PVC (**Figure 6F-G**). These data suggested that PIII surface treatment of PVC affected the orientation of the immobilized rDV core protein and the availability of the HS chains.

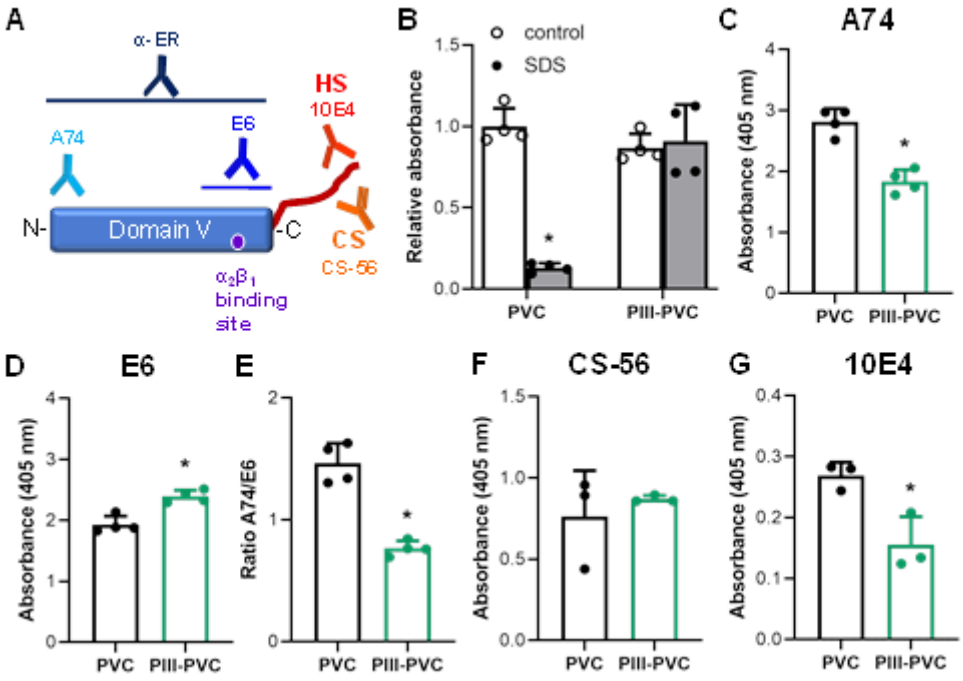

Figure 6. PIII treatment affects the orientation of rDV on PVC. (A) Schematic representation of the antibody epitopes for the protein core and GAG chains on rDV annotated with the $\alpha_2\beta_1$ integrin binding site. Antibody clones A74, E6, 10E4 and CS-56 are monoclonal antibodies while a-ER is a polyclonal antibody with epitopes located throughout domain V. **(B)** ELISA analysis of perlecan domain V protein epitopes available on rDV immobilized on either PVC or PIII-PVC detected using the rabbit polyclonal anti-endorepellin (recombinant perlecan domain V) antibody and observed prior to and following treatment with SDS to remove non-covalently bound protein. ELISA analysis of perlecan domain V protein epitopes available on rDV immobilized on either PVC or PIII-PVC detected using either **(C)** the monoclonal antibody clone A74 or **(D)** monoclonal antibody clone E6. **(E)** Ratio of absorbance values presented in (C) and (D). ELISA analysis of perlecan domain V GAG epitopes available on rDV immobilized on either PVC or PIII-PVC detected using either **(F)** monoclonal anti-CS antibody clone CS-56 or **(G)** monoclonal anti-HS antibody clone 10E4. Data are mean ± SD, *n*=3, *p*-values were calculated using one-way ANOVA with Tukey's test, **p*<0.05 compared to PVC.

To explore the effect of the GAGs on the orientation of immobilized rDV, the same experimental setup was employed to immobilize rDV treated to remove the GAG chains prior to exposure to PVC and PIII-PVC. SDS treatment confirmed that the rDV core protein was physisorbed on PVC and

robustly tethered to PIII-PVC with a similar level of rDV epitopes available on the surfaces before SDS treatment; suggestive of the same level of protein adsorption (**Figure 7A**). When the rDV core was immobilized on PVC it was orientated to expose more N-terminal epitopes (p=0.0010; **Figure 7B**) and less C-terminal epitopes (p=0.0010; **Figure 7C**) than on PIII-PVC. The ratio of absorbance values for the N- to C- terminal epitopes indicated that rDV core protein tethered to PVC favored exposure of the N-terminal epitopes while rDV core protein tethered to PIII-PVC favored exposure of the C-terminal epitopes (**Figure 7D**). Furthermore, comparison of the ratios of absorbance values for the N- to C- terminal epitopes for rDV and rDV core protein indicated that more C-terminal epitopes on rDV were exposed on PIII-PVC than when rDV core protein was immobilized on this surface (Figures 6E and 7D). However, the opposite occurred for rDV immobilized on PVC with more C-terminal epitopes exposed for rDV core on PVC than rDV. Together these data indicated that both the biomaterial surface and the presence of the GAG chains affected the orientation of immobilized rDV.

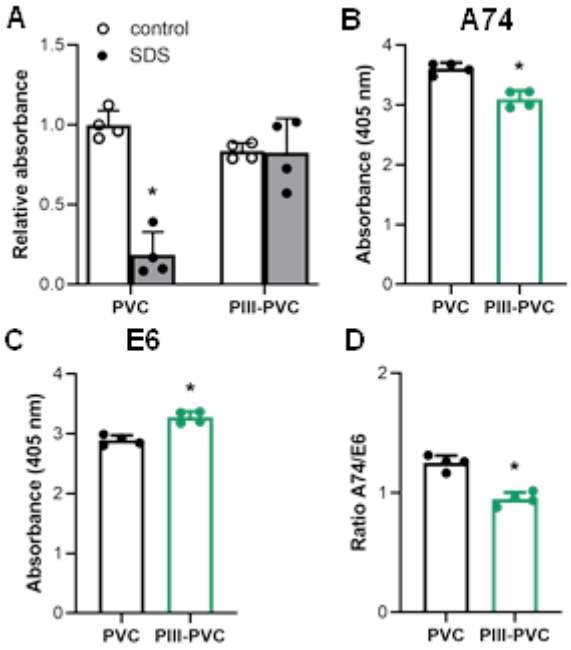

Figure 7. PIII treatment affects the orientation of rDV core on PVC. (A) ELISA analysis of perlecan domain V protein epitopes available on rDV core (rDV digested with both heparinase III and chondroitinase ABC to remove HS and CS, respectively) immobilized on either PVC or PIII-PVC detected using the rabbit polyclonal anti-endorepellin antibody raised against perlecan domain V and observed prior to and following treatment with SDS to remove non-covalently bound protein. ELISA analysis of perlecan domain V protein epitopes available on rDV immobilized on either PVC or PIII-PVC detected using either **(B)** the monoclonal antibody clone A74 or **(C)** monoclonal antibody clone E6. A schematic of the antibody epitopes in presented in Figure 6A. **(D)** Ratio of absorbance values presented in (B) and (C). Data are mean ± SD, n=4, p-values were calculated using one-way ANOVA with Tukey's test, *p<0.05 compared to PVC.

The bioactivity of tethered biomolecules is dependent on their orientation on the surface. Thus, platelet adhesion to the rDV biofunctionalized PVC and PIII-PVC was explored using platelets

suspended in a complex protein-containing solution, plasma/SSP, a buffer used for platelet storage prior to transfusion,[61] to establish the ability of rDV biofunctionalization to perform in a clinically relevant environment. PVC coated with albumin (negative control) supported the same level of platelet adhesion as uncoated PVC (p>0.05) while fibrinogen coated PVC (positive control) supported 3.4-fold more platelet adhesion than the pristine surface (p=0.0027) (**Figure 8A**). These data indicated that albumin did not reduce platelet adhesion to PVC when platelets were presented in the complex plasma protein-containing buffer, in contrast to when platelets were presented in the protein-free Tyrode's buffer (Figure 2B). To explore the effect of rDV immobilization on PVC and PIII-PVC, the number of platelets adhered to each surface was presented relative to uncoated PVC (control PVC) (**Figure 8B**). These data indicated that the physisorption of either albumin or rDV had no effect (p>0.05) on the level of platelet adhesion compared to control PVC. In addition, control PIII-PVC supported the same level of platelet adhesion as control PVC. However, rDV tethered to PIII-PVC supported 2.8-fold more platelet adhesion than control PIII-PVC (p = 0.0020). While rDV supported a similar or greater level of platelet adhesion than the control PVC or PIII-PVC, adhered platelets exhibited a lower level of spreading than on the control surfaces (p=0.0451 and 0.0013, respectively) (**Figure 8C**) indicative of a low level of platelet activation. Together, these data suggested that either rDV supported platelet adhesion due to its altered orientation on the PIII-PVC or that components of the plasma protein-containing buffer interacted with the immobilized rDV to support platelet adhesion.

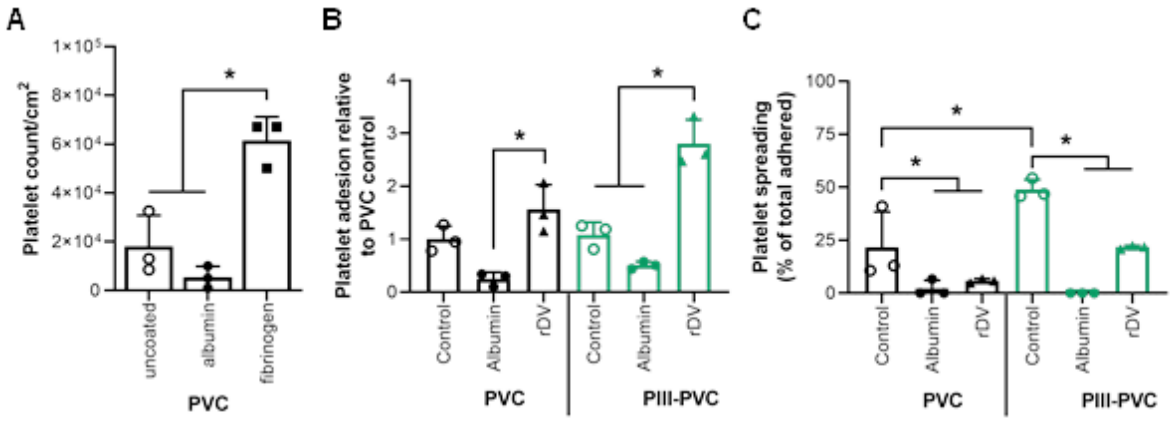

Figure 8. rDV biofunctionalization reduces platelet activation, but not adhesion, on PVC and PIII-PVC. (A) Platelet adhesion to PVC that was either uncoated or coated with albumin or fibrinogen via physisorption presented as the number of adhered platelets per cm^2. **(B)** Platelet adhesion to PVC or PIII-PVC that was either uncoated (Control) or biofunctionalized with albumin or rDV presented as fold change compared to PVC Control. **(C)** Proportion of adhered platelets with a spread morphology as determined by the presence of polymerize actin filaments. Platelets were suspended in plasma/SSP+ for exposure to the surfaces. Data are mean ± SD, *n*=3, *p*-values were calculated using one-way ANOVA with Tukey's test, **p*<0.05.

To explore the mechanism of platelet interaction with rDV immobilized on PVC and PIII-PVC, platelet adhesion was explored when platelets were presented in Tyrode's buffer in the absence of exogenous plasma proteins. The level of platelet adhesion to uncoated PVC and PIII-PVC was also analyzed by comparing the presentation of platelets in either Tyrode's buffer or plasma/SSP+ (**Figure 9A**). The level of platelet adhesion to PVC using platelets suspended in plasma/SSP+ was 11-fold less (*p*<0.0001) than when suspended in Tyrode's buffer and similarly for platelets exposed to PIII-PVC with 12-fold less platelet adhesion (*p*<0.0001). These data suggested that plasma proteins interacted

with PVC to alter platelet interactions. Albumin physisorbed on PVC (negative control) supported 13-fold less platelet adhesion than the pristine surface (p=0.0015) while fibrinogen coated PVC (positive control) supported 1.7-fold more platelet adhesion than the pristine surface (p=0.0070) (**Figure 9B**). These data established that the control proteins behaved in the same way as when physisorbed onto tissue culture plastic. To explore the effect of rDV immobilization on PVC and PIII-PVC, the number of platelets adhered to each surface was compared to uncoated PVC (control PVC) (**Figure 9C**). These data indicated that the physisorption of albumin, rDV or rDV core protein supported less platelet adhesion than control PVC (p<0.0001). Interestingly, uncoated PIII-PVC supported 3-fold more platelet adhesion than control PVC (p=0.0016). Furthermore, tethering of either albumin or rDV reduced platelet adhesion to PIII-PVC compared to the uncoated PIII-PVC with a 2.6- and a 3.6-fold reduction, respectively (p=0.0017 and 0.0007, respectively). However, rDV core protein immobilized on PIII-PVC supported platelet adhesion to the same extent as uncoated PIII-PVC (p>0.05) (**Figures 9C-D**). Platelet morphology was analyzed by quantifying the proportion of all adhered platelets that exhibited a spread morphology with polymerized actin filaments. This analysis indicated that platelets were less spread on protein coated PVC (p<0.0010) and either albumin or rDV biofunctionalized PIII-PVC than the uncoated surfaces (p=0.0020 and 0.0092, respectively) (**Figure 9E**). These data suggested that rDV did not support platelet adhesion or activation when tethered to PVC via physisorption or PIII surface treatment. Furthermore, the anti-adhesive property of rDV on PIII-PVC was dependent on the presence of the GAG chains.

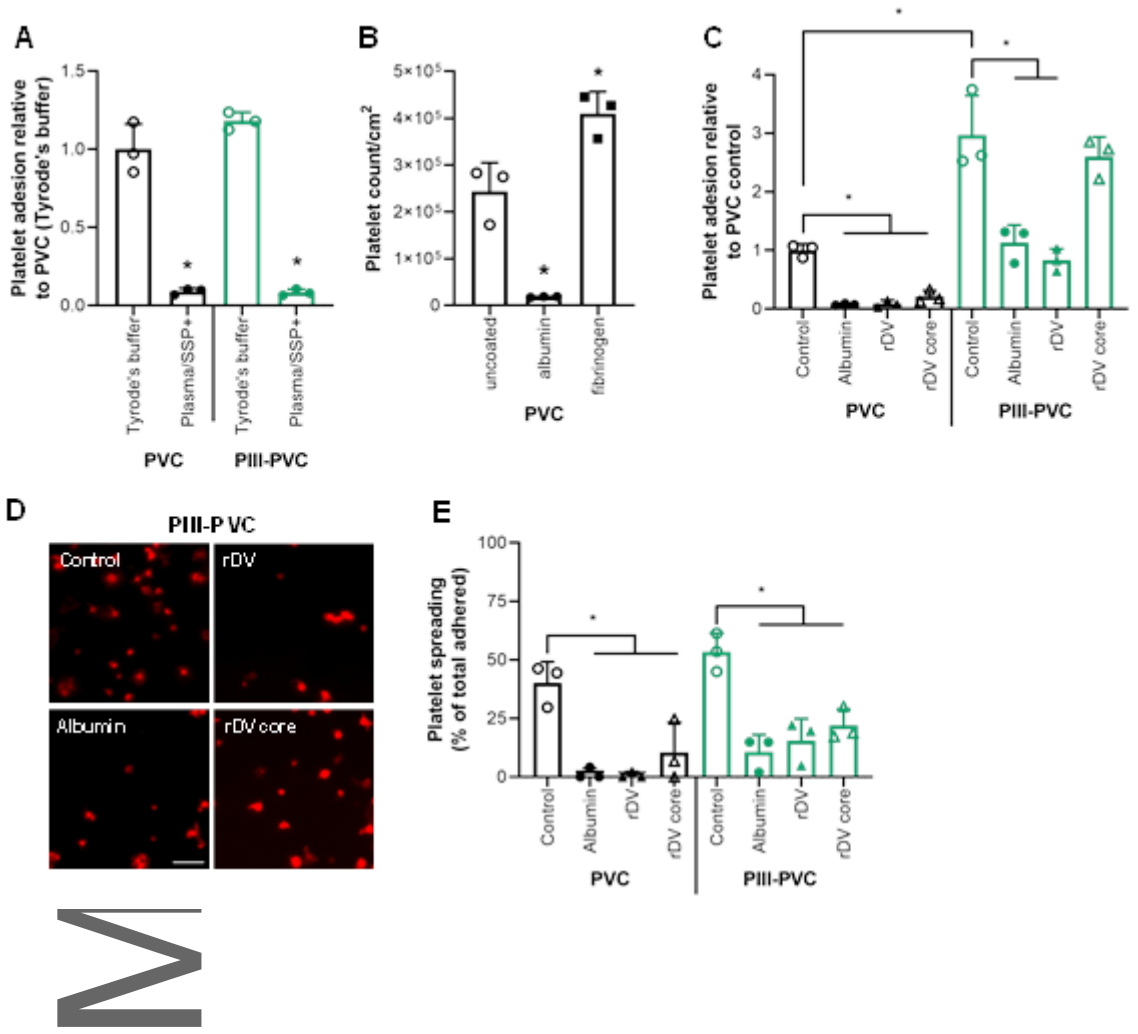

Figure 9. rDV biofunctionalization reduces platelet adhesion to PVC and PIII-PVC. (A) Platelet adhesion to PVC or PIII-PVC with platelet suspended in either Tyrode's buffer or plasma/SSP+ presented as fold change compared to PVC for platelets presented in Tyrode's buffer. Data are mean ± SD, *n*=3, *p*-values were calculated using one-way ANOVA with Tukey's test, **p*<0.05 compared to platelets in Tyrode's buffer adhered to PVC. **(B)** Platelet adhesion to PVC that was either uncoated or coated with albumin or fibrinogen via physisorption presented as the number of adhered platelets per cm^2 (platelets presented in Tyrode's buffer). Data are mean ± SD, *n*=3, *p*-values were calculated using one-way ANOVA with Tukey's test, **p*<0.05 compared to uncoated. **(C)** Platelet adhesion to PVC or PIII-PVC that was either uncoated (control) or biofunctionalized with albumin, rDV or rDV core presented as fold change compared to PVC control (platelets presented in Tyrode's buffer). Data are mean ± SD, *n*=3, *p*-values were calculated using one-way ANOVA with Tukey's test, **p*<0.05 compared to uncoated. **(D)** Representative images of platelets adhered to PIII-PVC biofunctionalized

with control, albumin, rDV or rDV core protein detected by fluorescence microscopy following actin staining using rhodamine phalloidin (platelets presented in Tyrode's buffer). Scale bar = 10 μm. **(E)** Proportion of adhered platelets with a spread morphology as determined by the presence of polymerized actin filaments. Data are mean ± SD, *n*=3, *p*-values were calculated using one-way ANOVA with Tukey's test, **p*<0.05.

3. Discussion

Perlecan, the major proteoglycan in the vascular basement membrane, is a promising bioactive for blood contacting applications due to its ability to support endothelial cell activities, but neither smooth muscle cell nor platelet adhesion.[31, 36, 47, 48] Perlecan is anti-adhesive to platelets in the presence of the GAG chains as shown here and previously[47] and does not support platelet activation either in the presence or absence of the GAG chains.[31, 47] Furthermore, perlecan can inhibit platelet factor 4-mediated platelet activation.[31] This study furthered the mechanistic understanding of platelet adhesion to perlecan and demonstrated that the protein core domains III and V were involved in platelet adhesion. Platelets have been reported to bind to perlecan via the $\alpha_2\beta_1$ integrin binding site located in domain V.[47, 62, 63] Recombinant forms of human perlecan domain V (rDV and endorepellin) are reported to support a low level of platelet adhesion and activation involving the $\alpha_2\beta_1$ integrin. [49, 62, 64] When the rDV core protein was presented here in the absence of GAG chains, it did not support platelet adhesion to the same extent as the perlecan core protein. This suggests that other regions of perlecan may act in concert to support platelet adhesion, such as domain III shown here for the first time, which are supported by previous studies implicating domains III and IV in cell adhesion.[36, 52]

Platelet adhesion to rDV was shown here to be independent of the GAG chain and platelets were not activated by rDV either in solution or when physisorbed, furthering the mechanistic understanding of platelet interactions with the C-terminal region of perlecan. The necessity for the GAG chains on perlecan to modulate platelet adhesion to the core protein [47] contrasts with the activities for rDV observed here. Thus, rDV is a promising biomolecule to tether to the surface of biomaterials to improve performance for blood-contacting applications for its ability to modulate vascular smooth muscle cell and platelet adhesion, as a precursor for thrombosis,[65] whilst supporting endothelial cell adhesion and surface endothelialization.[48]

PVC was modified with rDV via either physisorption or PIII treatment that yielded changes in the surface chemical bonds indicative of dry plasma surface modification as reported previously.[66] Surface modification with PIII treatment was also evident by a reduced water contact angle compared to PVC in agreement with previous reports where the DEHP plasticizer, incorporated via non-covalent interactions, increased the hydrophobicity of PVC.[66, 67] Surface wettability is influenced by the presence of hydrophobic bonds and surface roughness, [68] however, PIII treatment has a negligible effect on the surface roughness of water insoluble polymers as shown for PVC in this study, but affects surface chemistry.[69] Thus, the reduced water contact angle for PIII-PVC is indicative of a more hydrophilic surface than PVC and may be expected to result in less protein denaturation upon adsorption,[70] which may affect bioactivity. The free radicals present on the surface of PIII-treated biomaterials enable irreversible attachment of biomolecules[6] without the use of chemicals that may affect the cytocompatibility of the material and are able to retain bioactivity[6, 51] and are thus attractive for medical device applications.

Tethering of rDV to PVC was achieved via either physisorption or robust, SDS-resistant attachment via PIII treatment with both methods achieving the same level of binding. This finding agrees with the ability of PIII to enable robust attachment of rDV to silk fibroin[49, 51] as well as albumin or tropoelastin to various other biomaterial surfaces ensuring persistence of the coating in various environments.[37, 71, 72] Both methods of rDV tethering reduced platelet adhesion compared to the pristine PVC, however, the mechanisms were unique for each tethering method. Physisorption of rDV on PVC orientated the molecule to favor exposure of the N-terminus and hinder access to the $\alpha_2\beta_1$ integrin-binding region near the C-terminus which inhibited platelet adhesion, independent of the GAG chain. In contrast, PIII treatment orientated rDV to favor exposure of the C-terminus where the $\alpha_2\beta_1$ integrin binding site is located[63] that may reveal adhesive sites for platelets. Indeed, in the absence of GAG chains rDV tethered to PIII-PVC supported platelet adhesion, however, rDV did not support platelet adhesion to this surface when the GAG chains were present. Thus, rDV tethered to PIII-PVC reduced platelet adhesion via the GAG chains as reported for perlecan.[47, 48] The immobilization-dependent orientation of rDV has also been reported for silk fibroin where tethering via physisorption supported a higher level of platelet adhesion than rDV tethering via carbodiimide-based wet chemistry.[49] Differences in the orientation of antibodies physisorbed and covalently linked to PIII treated polycarbonate, favoring the variable region exposed on the PIII-treated surface, have also been reported.[73] This suggests that surface biofunctionalization and activity likely depends on a range of factors including the chemistry, surface charge, wettability and topography of the surface as well as the concentration, pH, temperature and ionic strength of the protein.[74, 75] Surface charge has been manipulated through the setting of pH in the immobilization solution to

control the orientation of approach of peptides. This orientation was then 'locked-in' by radical reactions that achieved covalent coupling to the surface.[76]

Analysis of platelet interactions in Tyrode's buffer with rDV tethered to PVC and PIII-PVC enabled analysis of the mechanisms by which the biofunctionalization was anti-adhesive to platelets. Analysis of platelet interactions in plasma/SSP+ enabled exploration of a more clinically relevant environment. Under these conditions, platelet adhesion to the pristine PVC was reduced, however, rDV lost its anti-adhesive effect for platelets with no effect compared to uncoated PVC and enhanced platelet adhesion to PIII-PVC compared to uncoated PIII-PVC. This somewhat contradictory result indicated that biofunctionalization with rDV likely enhanced interactions with the proteins present in plasma. Given the ability of perlecan to interact with many extracellular matrix proteins[77] and plasma proteins such as fibronectin[78], it is likely that rDV supports interactions with plasma proteins that presented an adhesive surface for platelets. This concept is worthy of future investigation. Interestingly, regardless of whether platelets were presented in plasma protein containing- or protein free-environments, the platelets that adhered to rDV functionalized PVC and PIII-PVC were not activated. This is an important finding in the pursuit of bioactive coatings for blood-contacting applications as platelet activation is a precursor to thrombosis, the loss of functional platelets and medical device failure. This study analyzed platelet interactions in static assays, while dynamic assays are warranted in future studies to resemble clinically relevant environments more closely. However, this study established rDV as a promising and versatile molecule to tether to both synthetic and natural biomaterials[49, 50] via either physisorption or

covalent methods to modulate vascular cell activities for blood contacting diagnostic and therapeutic applications.

4. Conclusion

Perlecan, a major component of the vascular basement membrane, was found to support low levels of platelet adhesion via domains III and V as well as the GAG chains. rDV presented benefits over perlecan as a coating for biomaterials with low platelet adhesion and less reliance on the GAG chains for bioactivity. Tethering of rDV to PVC via physisorption or covalent coupling enabled by PIII treatment determined the orientation of immobilized rDV and the mechanisms by which it reduced platelet adhesion compared to PVC. Importantly, irrespective of tethering method, rDV did not support platelet activation, a precursor for thrombosis and a major cause of blood-contacting device failure. Thus, biomaterial biofunctionalization with rDV is a promising platform for blood-contacting applications by virtue of its ability to tune platelet and other vascular cell activities.

5. Experimental Section

All reagents were purchased from Sigma-Aldrich unless stated otherwise.

Isolation of perlecan and recombinant human perlecan domain V (rDV): Perlecan was isolated from human coronary artery endothelial cells (Cell Applications, San Diego, CA, USA) via a two-step

process involving anion exchange chromatography using a diethylaminoethyl resin followed by immunoaffinity chromatography using a monoclonal anti-perlecan domain I antibody (clone A71) affinity column, as previously described.[79] rDV (amino acids 3611 to 4391 of human perlecan, accession P98160) was stably expressed by transfecting human embryonic kidney (HEK)-293 cells as previously described.[80] rDV was secreted into the medium and purified via anion exchange chromatography and found to be a proteoglycan decorated with chondroitin sulphate (CS) and heparan sulphate (HS) as previously described.[45] Protein concentration was determined by the Coomassie protein assay. The purity of the perlecan and rDV fractions was determined by mass spectrometry as described previously[81] (**Figure S3**).

Platelet isolation from human blood: All studies were conducted in accordance with protocols approved by the UNSW Sydney human ethics committee (reference HC14108). Platelets were obtained from Australian Red Cross Lifeblood as fresh platelet concentrates (300 mL; 2.4 x 10^{11} platelets mL^{-1} in 30 % plasma/ 70 % SSP+ (69.3 mM NaCl, 10.8 mM $C_6H_8O_7$, 32.5 mM NaOAc, 28.2 mM PO_4^{3-}, 5 mM K^+, 1.5 mM Mg^{2+}, pH 7.1; Macropharma, Mouvaux, France)). Platelets were diluted in either Tyrode's buffer (1.8 mM $CaCl_2$, 1 mM $MgCl_2$, 2.7 mM KCl, 136.9 mM NaCl, 0.4 mM NaH_2PO_4, 11.8 mM $NaHCO_3$, 5.6 mM glucose, 0.1 U mL^{-1} Apyrase, pH 7.4) or 30 % plasma/ 70 % SSP+ (plasma/SSP+) to 2 x 10^7 platelets mL^{-1} for experimentation.

Static platelet adhesion assays: Sixteen-well chamber slides (Nunc™ Lab-Tek™) were coated with proteins (50 µL; 10 µg mL^{-1} perlecan, 10 µg mL^{-1} rDV, 100 µg mL^{-1} bovine serum albumin (BSA;

negative control) or 30 µg mL^{-1} human fibrinogen (positive control); concentrations previously shown to form a monolayer on biomaterial surfaces[47, 56]) for 2 h at 37 °C. Where necessary, perlecan or rDV was digested with heparinase III (0.01 U mL^{-1}; EC 4.2.2.8, Iduron, Cheshire, UK) to remove HS, chondroitinase ABC (0.05 U mL^{-1}; EC 232-777-9, Seikagaku, Japan) to remove CS or both for 16 h at 37 °C before coating. Wells were washed twice with Dulbecco's phosphate buffered saline, pH 7.4 (PBS) and blocked with 1 % (w/v) BSA in PBS (50 µL) for 1 h at 37 °C. Wells were washed three times with PBS followed by the addition of platelet suspension (100 µL; 2 x 10^7 platelets mL^{-1}) to each well and incubated for 1 h at 37 °C. Non-adherent platelets were removed by two washes with PBS. Adherent platelets were fixed with 4 % (w/v) paraformaldehyde in PBS for 15 min at 37 °C and subsequently rinsed twice with PBS. Platelets were permeabilized with 300 mM sucrose, 50 mM NaCl, 3 mM $MgCl_2$, 2 mM HEPES, 0.5 % (v/v) Triton X-100, pH 7.2 for 5 min at 4 °C and blocked with 1 % (w/v) BSA in PBS for 1 h at room temperature. Wells were rinsed twice with PBS before staining with rhodamine phalloidin (1:200 dilution in 1 % (w/v) BSA/PBS) (Life Technologies, Carlsbad, CA, USA) for 1 h at room temperature in the dark. Samples were rinsed three times with PBS and covered with mounting medium (Prolong™ Gold Antifade Mountant, ThermoFisher Scientific, Australia). Platelets were visualized under a fluorescence microscope (Axioskop Mot Mat 2, Zeiss, Germany) with a 40x objective. The total platelet count and number of spread platelets were quantified from 5 fields of view per sample (n=3 samples per condition) using ImageJ (National Institutes of Health, USA).

To investigate the perlecan core protein regions involved in platelet adhesion using antibodies, perlecan was treated to remove HS as above before coating. Wells were then blocked with 1 % BSA in PBS for 1 h at 37 °C followed by the addition of mouse monoclonal anti-perlecan antibodies (2 µg

mL^{-1}) raised against domains I (clone A71, Abcam, Cambridge, MA, USA), III (clone 7B5, Abcam, Cambridge, MA, USA), IV (clone A7L6, Abcam, Cambridge, MA, USA) or V (clone A74, Abcam, Cambridge, MA, USA) for 1 h at 37 °C before rinsing twice with PBS and the addition of platelets in Tyrode's buffer.

To investigate the perlecan core protein regions involved in platelet adhesion using peptides (gift from Dr B. Oliver, University of Technology, Sydney, Sydney, NSW, Australia), perlecan was treated to remove HS as above before coating. Wells were then blocked with 1 % BSA in PBS for 1 h at 37 °C followed by the addition of peptides (10 μg mL^{-1}; **Table S1**) for 1 h at 37 °C before rinsing twice with PBS and the addition of platelets in Tyrode's buffer.

Platelet morphology visualized by scanning electron microscopy (SEM): Circular glass cover slips were coated with proteins, blocked with BSA and exposed to platelets suspended in Tyrode's buffer as above. The surfaces were washed three times with PBS and fixed with 2.5 % glutaraldehyde for 16 h at 4 °C followed by washing three times with PBS and dehydrating with increasing concentrations of ethanol (50 – 100 % (v/v)). Surfaces were dried using a critical point dryer (Autosamdri-815, Tousimis, MD, USA) and sputter coated (K550x, Emitech, France) with gold for 3 min. Platelets were subsequently visualized by SEM (S3400, Hitachi, Germany) at 1000x magnification.

Platelet activation by proteins in solution measured by flow cytometry: Platelet suspension (5 x 10^5 platelets mL^{-1}) diluted in Tyrode's buffer were exposed to adenosine diphosphate (ADP; 20 μM; positive control), BSA (100 μg mL^{-1}), fibrinogen (30 μg mL^{-1}), perlecan (10 μg mL^{-1}) or rDV (10 μg mL^{-1})

for 5 min at 37 °C, followed by the addition of phycoerythrin (PE) conjugated mouse anti-human CD62P (1 µg mL^{-1}; BD Biosciences, CA, USA) or fluorescein isothiocyanate (FITC) labeled mouse anti-human PAC-1 (1 µg mL^{-1}; BD Biosciences, CA, USA) for 20 min at room temperature in the dark. This reaction was stopped by the addition of 1 % (w/v) paraformaldehyde. The fluorescence intensity of 10,000 platelets was analyzed in a flow cytometer (BD, FACScan, CA, USA).

Platelet adhesion and activation by immobilized proteins measured by quartz crystal microbalance with dissipation monitoring (QCM-D): A continuous flow (0.2 mL min^{-1}) and temperature of 37 °C was applied throughout the experiments using a QCM-D (Analyzer, Q-Sense). After a baseline was established with PBS (pH 7.4, filtered and degassed), the sensor surfaces were coated with proteins (BSA (100 µg mL^{-1}), fibrinogen (30 µg mL^{-1}), perlecan (10 µg mL^{-1}) or rDV (10 µg mL^{-1})), rinsed with PBS to remove unbound protein and blocked with 1 % BSA/PBS (300 µL) to avoid non-specific platelet interactions. A rinse with PBS was performed before the introduction of platelet suspension (5 mL; 2 x 10^7 platelets mL^{-1} in Tyrode's buffer) for 20 min and a final rinse with PBS. The binding events were monitored by changes in frequency (Δf) and dissipation (ΔD) at the fundamental frequency as well as the 3^{rd}-11^{th} overtones. The protein coatings were established to be stable over the analysis period.[47, 55]

PVC surface characterization and modification via plasma immersion ion implantation (PIII): Platelet storage bags (PVC; Terumo BCT Teruflex®, Terumo, CO, USA) imaged under an optical microscope

(Contour GT-I ® 3D, Bruker, MA, USA) in vertical scanning interferometry mode using a 20x objective, green illumination and a threshold of 0.001 %.

For plasma immersion ion implantation (PIII), PVC samples (2 x 5.5 cm) were mounted onto a metal substrate holder, with a metallic mesh placed 5 cm in front of the sample holder.[37] The substrate holder was placed into the vacuum chamber and evacuated to a base pressure of 10^{-5} Torr, with N_2 gas introduced with a flow rate of ~72 standard cubic centimeters (sccm) to a pressure of 2 x 10^{-3} Torr. The source of ions for PIII treatment was an inductively coupled RF plasma (13.56 MHz), with a forward power of 100 W and a reverse power of 12 W. Acceleration of plasma ions was achieved with 20 kV bias pulses of 20 µs, applied to the substrate holder and mesh, at a frequency of 50 Hz for 800 s. The sample holder was earthed between pulses. PIII treated PVC samples were stored for 1 week at room temperature before use as our prior research indicated this to be the time required for the surface energy to stabilize whilst maintaining the radical flux to achieve protein attachment [82, 83].

The contact angle of PVC and PIII treated PVC (PIII-PVC) was measured at room temperature by placing the polymer films on a flat bench and adding a drop of deionized water (10 µL). Images of water droplets on each polymer surface were captured using a macrolens attached to a smartphone. The contact angle was measured by using the angle plug-in on ImageJ (National Institutes of Health, USA). Surface chemistry was assessed by attenuated total reflectance Fourier-transform infrared spectroscopy (ATR-FTIR; Alpha-P, Bruker, MA, USA). ATR-FTIR spectra were measured at 4 cm^{-1} resolution with 50 scans over the range of 400 – 4000 cm^{-1}.

Strength of rDV binding to PVC and PIII-PVC: PVC and PIII-PVC were coated with rDV (50 µL, 10 µgmL^{-1}) for 2 h at 37 °C. Where necessary, rDV samples were treated to remove HS and CS before coating. Wells were washed twice with PBS before the addition of 2 % (w/v) SDS for 1 h at 90 °C. Following the SDS wash, wells were rinsed four times with PBS and blocked with 0.1 % (w/v) casein for 1 h at room temperature. Wells were then washed twice with PBS containing 0.05 % (w/v) Tween-20 (PBS-T) and incubated with rabbit polyclonal anti-endorepellin antibody (α-ER; 50 µL; anti-perlecan domain V antibody, Dr R. Iozzo, Thomas Jefferson University, PA, USA) diluted in 0.1 % (w/v) casein for 2 h at room temperature. Wells were washed twice with PBS-T and incubated with biotinylated goat anti-rabbit secondary antibody (50 µL; Life Technologies, Carlsbad, CA, USA) diluted in 0.1 % (w/v) casein for 1 h at room temperature. Wells were then washed twice with PBS-T and incubated with horseradish peroxidase conjugated streptavidin (50 µL; SA-HRP, 1:500 in 0.1 % (w/v) casein; GE Healthcare, Little Chalfront, UK) for 30 min at room temperature. Wells were washed four times with PBS-T and 2,2'-Azino-bis(3-ethylbenzothiazoline-6-sulfonic acid) diammonium salt (100 µL; ABTS) was added to each well. The absorbance of the solution was read at 405 nm in a plate reader (Infinite® 200 Pro, Tecan, Switzerland).

rDV orientation on PVC and PIII-PVC: rDV was coated onto PVC or PIII-PVC as above. Immobilized rDV was probed with mouse monoclonal antibodies against the core protein (clones A74 and E6; 2 µg mL^{-1}, Abcam, Cambridge, MA, USA and Santa Cruz Biotechnology, Dallas, TC, USA, respectively), CS (clone CS-56; 2 µg mL^{-1}) or HS (clone 10E4; 2 µg mL^{-1}; US Biological, Salem, MA, USA) as previously described.[36]

Statistical analysis: All results were presented as mean ± standard deviation (SD). Sample size is indicated in each figure legend. For normally distributed data sets with equal variances, one-way ANOVA testing followed by a Tukey post-hoc test was carried out across groups. In all cases, significance was defined as $p \leq 0.05$. Statistical analysis was carried out using GraphPad Prism version 9 (GraphPad Software, USA).

Supporting Information

Supporting Information is available from the Wiley Online Library.

Acknowledgements

We would like to acknowledge funding support from the Australian Research Council, DP150104242 (MSL, JMW and JR-K), LP140101056 (MSL, JMW and DI) and FL190100216 (MMB). KC, KL and HNK were supported by the Australian Government Research Training Program Scholarships. JR-K was supported by the Heart Foundation of Australia Future Leader Fellowship (101896). SEM analysis was performed at the Electron Microscope Unit (EMU), mass spectrometry was performed at the Bioanalytical Mass Spectrometry Facility (BMSF) and QCM-D was performed at the Molecular Surface Interaction (MSI) Network Lab. EMU and BMSF are part of the Mark Wainwright Analytical Center at UNSW Sydney, which, in addition to MSI (ZE), is in part-funded by the Research Infrastructure program at UNSW. The authors thank Dr Sydney Liu at BMSF for performing mass spectrometry analysis. Australian governments fund Australian Red Cross Lifeblood to provide blood, blood products and services to the Australian community.

* corresponding author

deceased

Received: ((will be filled in by the editorial staff))
Revised: ((will be filled in by the editorial staff))
Published online: ((will be filled in by the editorial staff))

References

[1] C.D. Spicer, E.T. Pashuck, M.M. Stevens, *Chem. Rev.* **2018**, *118*, 7702.

[2] J.A. Shadish and C.A. DeForest, *Matter* **2020**, *2*, 50.

[3] F. Rusmini, Z. Zhong, J. Feijen, *Biomacromolecules* **2007**, *8*, 1775.

[4] C.J. Wilson, R.E. Clegg, D.I. Leavesley, M.J. Pearcy, *Tissue Eng.* **2005**, *11*, 1.

[5] S.L. Hirsh, D.R. McKenzie, N.J. Nosworthy, J.A. Denman, O.U. Sezerman, M.M. Bilek, *Colloids Surf. B: Biointerfaces* **2013**, *103*, 395.

[6] M.M. Bilek, D.V. Bax, A. Kondyurin, Y. Yin, N.J. Nosworthy, K. Fisher, A. Waterhouse, A.S. Weiss, C.G. dos Remedios, D.R. McKenzie, *Proc. Natl. Acad. Sci. U S A.* **2011**, *108*, 14405.

[7] M.M. Bilek and D.R. McKenzie, *Biophys. Rev.* **2010**, *2*, 55.

[8] S. Lakshmi and A. Jayakrishnan, *Artif. Organs* **1998**, *22*, 222.

[9] C.G. Feit, M.K. Chug, E.J. Brisbois, *ACS Appl. Bio Mater.* **2019**, *2*, 4335.

[10] K.Z. Hong, *J. Vinyl Addit. Technol.* **1996**, *2*, 193.

[11] B. Branger, M. Garreau, G. Baudin, J.C. Gris, *Artif. Organs* **1990**, *13*, 697.

[12] J.L. Brash, T.A. Horbett, R.A. Latour, P. Tengvall, *Acta Biomater.* **2019**, *94*, 11.

[13] J. Storck, H.A. Del Razek, E.R. Zimmermann, *Biomaterials* **1996**, *17*, 1791.

[14] A. de Mel, G. Jell, M.M. Stevens, A.M. Seifalian, *Biomacromolecules* **2008**, *9*, 2969.

[15] W. Gao, T. Lin, T. Li, M. Yu, X. Hu, D. Duan, *Int. J Clin. Exp. Med.* **2013**, *6*, 259.

[16] D.M. Eckmann, I.Y. Tsai, N. Tomczyk, J.W. Weisel, R.J. Composto, *Colloids Surf. B: Biointerfaces* **2013**, *108*, 44.

[17] Y. Zou, B.F. Lai, J.N. Kizhakkedathu, D.E. Brooks, *Macromol. Biosci.* **2010**, *10*, 1432.

[18] B. Balakrishnan and A. Jayakrishnan, *Trends Biomater. Artif. Organs* **2005**, *18*, 230.

[19] W. Zhang, P.K. Chu, J. Ji, Y. Zhang, X. Liu, R.K. Fu, P.C. Ha, Q. Yan, *Biomaterials* **2006**, *27*, 44.

[20] L. Peng and C. Yashao, *Plasma Sci. Technol.* **2004**, *6*, 2328.

[21] D.J. Balazs, K. Triandafillu, P. Wood, Y. Chevolot, C. van Delden, H. Harms, C. Hollenstein, H.J. Mathieu, *Biomaterials* **2004**, *25*, 2139.

[22] R. Almouse, X. Wen, S. Na, G. Anderson, D. Xie, *Polym. Adv. Technol.* **2018**, *30*, 1216.

[23] R. Almouse, X. Wen, S. Na, G. Anderson, D. Xie, *J. Biomater. Appl.* **2019**, *33*, 1415.

[24] X. Wen, R. Almouse, G. Anderson, S. Na, D. Xie, *J. Biomater. Sci. Polym. Ed.* **2019**, *30*, 322.

[25] X. Li, J.H. Wang, Z.C. Tang, R. Chen, J.Y. Fang, D. Li, H. Chen, *Acta Polym. Sin.* **2020**, *51*, 1248s.

[26] J. Ji, Q. Tan, J. Shen, *Polym. Adv. Technol.* **2004**, *15*, 490.

[27] A. Asadinezhad, I. Novák, M. Lehocký, F. Bílek, A. Vesel, I. Junkar, P. Sáha, A. Popelka, *Molecules* **2010**, *15*, 1007.

[28] C. Mao, W.B. Zhao, A.P. Zhu, J. Shen, S.C. Lin, *Process Biochem.* **2004**, *39*, 1151.

[29] A. Waterhouse, S.G. Wise, M.K.C. Ng, A.S. Weiss, *Tissue Eng. B* **2011**, *17*,

[30] K.A. Woodhouse, P. Klement, V. Chen, M.B. Gorbet, F.W. Keeley, R. Stahl, J.D. Fromstein, C.M. Bellingham, *Biomaterials* **2004**, *25*, 4543.

[31] M.S. Lord, B. Cheng, B.L. Farrugia, S. McCarthy, J.M. Whitelock, *J. Biol. Chem.* **2017**, *292*, 4054.

[32] S.P. Vyas and B. Vaidya, *Expert Opin Drug Deliv* **2009**, *6*, 499.

[33] B.L. Farrugia, K. Chandrasekar, L. Johnson, J.M. Whitelock, D.C. Marks, D.O. Irving, M.S. Lord, *Biointerphases* **2016**, *11*, 029701.

[34] D.M. Hylton, S.W. Shalaby, R.A. Latour Jr., *J. Biomed Mater. Res. A* **2005**, *73A*, 349.

[35] S.L. Goodman, S.L. Cooper, R.M. Albrecht, *J. Biomat. Sci. Polym. Ed.* **1991**, *2*, 147.

[36] M.S. Lord, C.Y. Chuang, J. Melrose, M.J. Davies, R.V. Iozzo, J.M. Whitelock, *Matrix Biol.* **2014**, *35*, 112.

[37] A. Kondyurin, K. Lau, F. Tang, B. Akhavan, W. Chrzanowski, M.S. Lord, J. Rnjak-Kovacina, M.M. Bilek, *ACS Appl. Mater. Interfaces* **2018**, 17605.

[38] R. Biran and D. Pond, *Adv. Drug Deliv. Rev.* **2017**, *112*, 12.

[39] M.K. Lazarides, C. Argyriou, G.A. Antoniou, E. Georgakarakos, G.S. Georgiadis, *Semin. Vasc. Surg.* **2016**, *29*, 192.

[40] S. Gore, J. Andersson, R. Biran, C. Underwood, J. Riesenfeld, *J. Biomed. Mater. Res. B Appl. Biomater.* **2014**, *102*, 1817.

[41] J.K. Burgess and B.H. Chong, *Eur. J. Haematol.* **1997**, *58*, 279.

[42] M. Costell, E. Gustafsson, A. Aszódi, M. Mörgelin, W. Bloch, E. Hunziker, K. Addicks, R. Timpl, R. Fässler, *J. Cell Biol.* **1999**, *147*, 1109.

[43] R.V. Iozzo, I.R. Cohen, S. Grassel, A.D. Murdoch, *Biochem. J.* **1994**, *302*, 625.

[44] D. Aviezer, D. Hecht, M. Safran, M. Eisinger, G. David, A. Yayon, *Cell* **1994**, *79*, 1005.

[45] J. Rnjak-Kovacina, F. Tang, X. Lin, J.M. Whitelock, M.S. Lord, *Biotechnol. J.* **2017**, *12*, 1700196.

[46] S.M. Knox and J.M. Whitelock, *Cell. Mol. Life Sci.* **2006**, *63*, 2435.

[47] M.S. Lord, B. Cheng, S.J. McCarthy, M. Jung, J.M. Whitelock, *Biomaterials* **2011**, *32*, 6655.

[48] M.S. Lord, W. Yu, B. Cheng, A. Simmons, L. Poole-Warren, J.M. Whitelock, *Biomaterials* **2009**, *30*, 4898.

[49] J. Rnjak-Kovacina, F. Tang, J.M. Whitelock, M.S. Lord, *Colloids Surf. B: Biointerfaces* **2016**, *148*, 130.

[50] X. Lin, F. Tang, S. Jiang, H. Khamis, A. Bongers, J.M. Whitelock, M.S. Lord, J. Rnjak-Kovacina, *Adv. Sci.* **2020**, *7*, 2000900.

[51] K. Lau, A. Waterhouse, B. Akhavan, L. Gao, H. Kim, F. Tang, J.M. Whitelock, M.M. Bilek, M.S. Lord, J. Rnjak-Kovacina, *Acta Biomater.* **2021**, *https://doi.org/10.1016/j.actbio.2021.02.014*,

[52] M.C. Farach-Carson, A.J. Brown, M. Lynam, J.B. Safran, D.D. Carson, *Matrix Biol.* **2008**, *27*, 150.

[53] Q. Lu and R.A. Malinauskas, *Artif. Organs* **2011**, *35*, 137.

[54] S.J. Shattil, J.A. Hoxie, M. Cunningham, L.F. Brass, *J. Biol. Chem.* **1985**, *260*, 11107.

[55] M.S. Lord, J.M. Whitelock, A. Simmons, R.L. Williams, B.K. Milthorpe, *Biointerphases* **2014**, *9*, 041002.

[56] M.S. Lord, C. Modin, M. Foss, M. Duch, A. Simmons, F.S. Pedersen, B.K. Milthorpe, F. Besenbacher, *Biomaterials* **2006**, *27*, 4529.

[57] J. Fatisson, S. Mansouri, D. Yacoub, Y. Merhi, M. Tabrizian, *J. R. Soc. Interface* **2011**, *8*, 988.

[58] C.A. Labarrere, A.E. Dabiri, G.S. Kassab, *Front. Bioeng. Biotechnol.* **2020**, *8*, 123.

[59] D.V. Bax, D.R. McKenzie, A.S. Weiss, M.M. Bilek, *Acta Biomater.* **2009**, *5*, 3371.

[60] D.V. Bax, D.R. McKenzie, A.S. Weiss, M.M. Bilek, *Biomaterials* **2010**, *31*, 2526.

[61] C. Saunders, G. Rowe, K. Wilkins, S. Holme, P. Collins, *Vox Sang.* **2011**, *101*, 112.

[62] G. Bix, J. Fu, E.M. Gonzalez, L. Macro, A. Barker, S. Campbell, M.M. Zutter, S.A. Santoro, J.K. Kim, M. Höök, C.C. Reed, R.V. Iozzo, *J. Cell Biol.* **2013**, *201*, 641.

[63] B.P. Woodall, A. Nyström, R.A. Iozzo, J.A. Eble, S. Niland, T. Krieg, B. Eckes, A. Pozzi, R.V. Iozzo, *J. Biol. Chem.* **2008**, *283*, 2335.

[64] G. Bix, R.A. Iozzo, B. Woodall, M. Burrows, A. McQuillan, S. Campbell, G.B. Fields, R.V. Iozzo, *Blood* **2007**, *109*, 3745.

[65] B. Nieswandt, I. Pleines, M. Bender, *J. Thromb. Haemost.* **2011**, *9 Suppl 1*, 92.

[66] A. Kondyurin, N.J. Nosworthy, M.M. Bilek, *Langmuir* **2011**, *27*, 6138.

[67] J.M. Hankett, W.R. Collin, Z. Chen, *J. Phys. Chem. B* **2013**, *117*, 16336.

[68] I.V. Pukhova, I.A. Kurzina, K.P. Savkin, O.A. Laput, E.M. Oks, *Nucl. Instrum. Methods Phys. Res. B* **2017**, *399*, 28.

[69] E.L. Snyder, M. Ezekowitz, R. Aster, S. Murphy, P. Ferri, E. Smith, L. Rzad, W. Davisson, C. Pope, R. Kakaiya, et al., *Transfusion* **1985**, *25*, 209.

[70] K. Nakanishi, T. Sakiyama, K. Imamura, *J. Biosci. Bioeng.* **2001**, *91*, 23.

[71] E.A. Wakelin, G.C. Yeo, D.R. McKenzie, M.M.M. Bilek, A.S. Weiss, *APL Bioeng.* **2018**, *2*, 026109.

[72] A. Kondyurin, K. Tsoutas, Q.-X. Latour, M.J. Higgins, S.E. Moulton, D.R. McKenzie, M.M. Bilek, *ACS Biomater. Sci. Eng.* **2017**, *3*, 2247.

[73] E. Kosobrodova, R. Jones, A. Kondyurin, W. Chrzanowski, P. Pigram, D. McKenzie, M. Bilek, *Acta Biomater.* **2015**, *19*, 128.

[74] M. Rabe, D. Verdes, S. Seeger, *Adv. Colloid Interface Sci.* **2011**, *162*, 87.

[75] S. Chen, L. Liu, J. Zhou, S. Jiang, *Langmuir* **2003**, *19*, 2859.

[76] L.J. Martin, B. Akhavan, M.M. Bilek, *Nat. Commun.* **2018**, *9*, 357.

[77] G. Bix and R.V. Iozzo, *Microsc. Res. Tech.* **2008**, *71*, 339.

[78] A. Heremans, B. De Cock, J.J. Cassiman, H. Van den Berghe, G. David, *J. Biol. Chem.* **1990**, *265*, 8716.

[79] J.M. Whitelock, L.D. Graham, J. Melrose, A.D. Murdoch, R.V. Iozzo, P.A. Underwood, *Matrix Biol.* **1999**, *18*, 163.

[80] M. Jung, M.S. Lord, B. Cheng, J.G. Lyons, H. Alkhouri, J.M. Hughes, S.J. McCarthy, R.V. Iozzo, J.M. Whitelock, *J. Biol. Chem.* **2013**, *288*, 3289.

[81] M.S. Lord, A.J. Day, P. Youssef, L. Zhuo, H. Watanabe, B. Caterson, J.M. Whitelock, *J. Biol. Chem.* **2013**, *288*, 22930.

[82] E.A. Kosobrodova, A.V. Kondyurin, K. Fisher, W. Moeller, D.R. McKenzie, M.M.M. Bilek, *Nucl. Instrum. Methods Phys. Res. B* **2012**, *280*, 128.

[83] E.A. Wakelin, M.J. Davies, M.M. Bilek, D.R. McKenzie, *ACS Appl Mater Interfaces* **2015**, *7*, 026109.

Summary

The use of polyvinyl chloride (PVC) for blood-contacting applications is limited as it supports thrombosis. This study explores the immobilization of recombinant human perlecan domain V on PVC, a proteoglycan that modulates vascular cell activity, via either physisorption or covalent attachment and reveals a promising platform for blood contacting applications by virtue of its ability to tune platelet activities.